Design and experimental validation of a magnetic device for stem cell culture

Rubén Salvador-Clavell[1], José-Manuel Rodríguez-Fortún[2], Irene López[2], José Javier Martín de Llano[1,3], Javier Orús[2], María Sancho-Tello[1,3], Carmen Carda[1,3,4], Mohamed H. Doweidar[4,5,6,*]

[1]Departamento de Patología, Facultad de Medicina y Odontología, Universitat de València, València 46010, Spain;
[2]Instituto Tecnológico de Aragón (ITAINNOVA), Zaragoza 50018, Spain;
[3]INCLIVA Biomedical Research Institute, València 46010, Spain;
[4]Centro de Investigación Biomédica en Red en Bioingeniería, Biomateriales y Nanomedicina (CIBER-BBN), Spain;
[5]Mechanical Engineering Department, University of Zaragoza, Zaragoza 50018, Spain;
[6]Aragon Institute of Engineering Research (I3A), University of Zaragoza, Zaragoza 50018, Spain.
* Corresponding author: mohamed@unizar.es

ABSTRACT

Cell culture of bone and tendon tissues requires a mechanical stimulation of the cells in order to mimic their physiological state. In the present work, a device has been conceived and developed to generate a controlled magnetic field with a homogeneous gradient in the working space. The design requirement was to maximize the magnetic flux gradient assuring a minimum magnetizing value in a 15 mm x 15 mm working area, which highly increases the normal operating range of this sort of devices. The objective is using the machine for two types of biological tests: magnetic irradiation of biological samples and force generation on paramagnetic particles embedded in scaffolds for cell culture. The device has been manufactured and experimentally validated by evaluating the force exerted on magnetic particles in a viscous fluid. Apart from the magnetic validation, the device has been tested for irradiating biological samples. In this case, *in vitro*, human dental pulp stem cells (hDPSC) viability has been studied after electromagnetic field exposition using the designed device. After 3 days of irradiation treatment, cellular microtissues showed a 59 % increase in viable cell number. Irradiated cells did not show morphological differences when compared with control cells.

INTRODUCTION

Several options can be found in the bibliography for the mechanical stimulation of living cells [1]: electromagnetic, electrostatic, mechanical and rotating magnetic fields among others [2,3]. The efficiency of electromagnetic field has been proved in clinical approach, and this clinical use has been approved by U.S. Food and Drug Administration (FDA) for cervical fractures regeneration [4]. In this line, the use of electromagnetic fields (EMF) [5,6] and remotely generate forces by these EMF [7] for biological applications is not new and has been proved to have a moderate impact on the cells [8]. It has been shown that EMF applications can improve *in vitro* cellular differentiation of mesenchymal stem cells (MSC) into cellular chondrogenic lineage for bone and cartilage regeneration [9,10]. On the other hand, electromagnetic stimulation could improve cellular proliferation, and in fact a 20 % increase has been shown when dynamic electromagnetic-mechanical stimulation was applied on cellular cultures [11].

The present work is focused on the design of a magnetic device for generating a magnetic flux pattern with homogeneous gradient that can be both used for irradiating biological samples or generating forces on embedded paramagnetic particles.

There are different designs in the literature for specific applications, being the results very much dependent on the objective magnetic patterns. In all the cases, external coils generate a magnetic flow through a circuit of low reluctance, which aligns the flow for creating a magnetic flow pattern with a controlled gradient in the working space. Most of the concepts use ferromagnetic or superparamagnetic particles for generating forces in presence of the gradient in the magnetic flux density. In the present work, for the design of the device, a regular gradient of 30 T/m in the working area of 15x15 mm is fixed as objective. The relatively large size of the working area makes the design specially challenging taking into account the high resulting reluctance in the gap and the need for an economical and power efficient solution. The former requires that the design can be done with standard materials and components; and the latter is a consequence of the need of not warming the biological sample, as it could therefore be damaged, and avoiding the use of complex cooling systems that would make difficult the installation of the device in the lab facilities.

Among the existing bibliography, there are interesting designs of magnetic tweezers to be remarked. The simple 1 pole design in [12] applies a magnetic field on a working area of 5.5 mm of diameter and obtained forces in the order of 3 pN with Dynabead M-450. This should correspond to a magnetic gradient of about 1000 T/m. De Vries *et al.* [13] developed a device with three poles that creates a gradient by generating magnetic flows in opposite directions at the same time. This device can produce forces in the range of around 1 nN with 2.8 µm M280 Dynal

in a working area of 20x20 µm (magnetic gradient of about 30000 T/m). A similar magnetic design with three poles is described in [14] for a workspace of 40x40x20 µm. Zhang *et al.* [15] describes a four pole device working on a 0.8x0.8 mm area. This design permitted changing the magnetic flux gradient by controlling the 4 coils. Besides, Huang *et al.* [16] extended the concept previously published [13] with two levels of poles to obtain a 3D actuation. They obtained a magnetic gradient over 40 T/m in an area of 0.5x0.5 mm. Two-dimensional forces have also been reported to move and rotate particles of 3 µm diameter with a magnetic gradient of 10 to 20 T/m with poles placed at a distance of 7.5 mm [17], although the control area is limited at a range of 50 µm from the center. Haber *et al.* [18] present a concept that can work in a much larger working area. It considers separated magnetizing and gradient coils. The former ones assure a minimum magnetizing field and the second ones are responsible for generating the gradient. The design obtained good results over a large area: a magnetic flux gradient ranging from 40 T/m to 100 T/m in a working gap among 15 and 20 mm. However, this design has a power consumption in the order of 9 kW, which had to be cooled using a water circuit.

The concept designed in the present work also has a wide operating range. It has a working area of 15x15 mm and can produce magnetic gradients in the order of 30 T/m. These requirements constrain the magnetic, electronic and mechanical designs of the actuator, as it has to work with high currents and, at the same time, it has to minimize the power consumption to reduce the risk of heating the biological samples. These conditions are fulfilled by optimizing the magnetic circuit and moving away the coils in order to reduce the losses and limiting the heat from the coils reaching the sample. Compared to [18], which is the device with more similar working areas, the proposed device works with much lower power consumptions and does not need special cooling elements.

The device has been tested on biological samples, human dental pulp stem cells (hDPSC). They are MSC that reside in the perivascular niche of the dental pulp [19]. This type of cells is easily obtained from extracted molars and can be differentiated *in vitro* into different cell types (including adipocytes, chondrocytes or osteoblasts) if specific conditions, as chemical substances or electromagnetic stimuli, are applied [20]. The designed device has been tested on hDPSC *in vitro* for analyzing cell viability when cultured microtissues were exposed to the electromagnetic field. The results show that using the device, increases the viable cell number.

The document is organized as follows. First, the design of the device and its validation is described. After that, the details of the biological experiment are given and the results of the test using the designed device are presented. Finally, the conclusions of the work are summarized.

MATERIAL AND METHODS

Description of the device

In this section, the design process and the final concept for the magnetic field generator is described.

Design of the magnetic device and experimental results

For the design of the magnetic device, we have followed a model-based approach following the typical V-methodology for mechatronic devices [21]. As it is described in Figure 1, starting from the initial system requirements, several concepts have been generated and compared by using Finite Element (FE) models as a basis for predicting their performance. Once the fittest option has been chosen, the detailed component design has started. As it will be described in the section results, the different parts of the device have been tested and evaluated prior to its final assembly and the validation of the complete system.

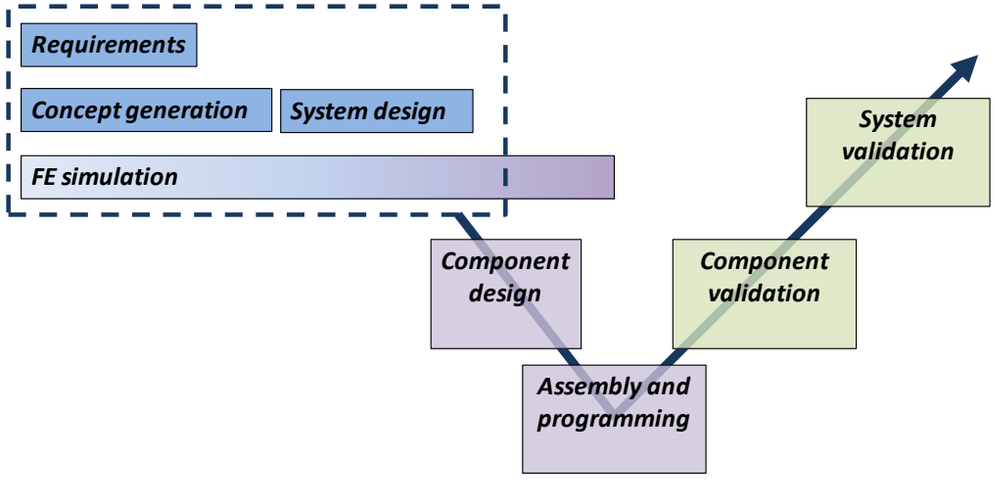

Figure 1. Design methodology.

Concept generation

The main requirements defined for the device were:

- its capability for generating a magnetic flux pattern with homogeneous gradient that can be both used for irradiating biological samples or generating forces on embedded paramagnetic particles,
- the sense of the magnetizing field should be variable, in order to produce forces in both directions,
- operating range of 15x15 mm,

- reaching at a regular gradient level of 30 T/m in the operating area, which is a representative value considering the magnetic tweezers described in the literature for mm-range devices [13,17,18] (this means force levels higher than 10 nN for nanoparticles of 40 µm of diameter and 5 % of ferrite material, which will be used to verify the performance of the device in the results section),
- use of standard magnetic materials for reducing the cost avoiding special materials (M330 - 50 A),
- separation of the coils from the samples for avoiding affecting them derived from the heat.

Figure 2 shows the main concepts of the design process. It includes the most representative intermediate progressions, which were mostly used to optimize the geometry in order to minimize the magnetic losses.

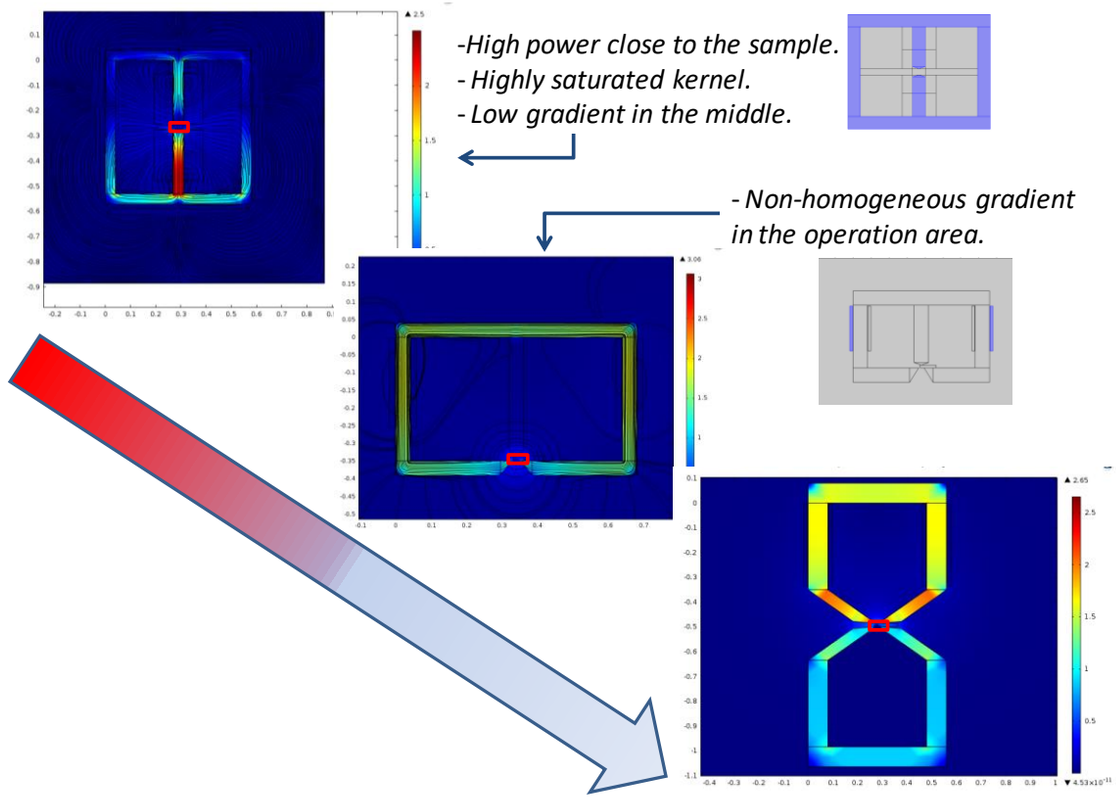

Figure 2. Concept evolution (framed in red, the operation area).

The initial approach on the top left-hand side of the figure was based on [18]. The design required high power (above 400 W at each gradient coil), a cooling system and the use of special material (Permandur 2V) due to the saturated kernel. Apart from that, the design did not obtain the

desired homogeneous field distribution in the operation range (specially at the center line as it appears in Figure 3). As in [18], the approach used a double set of coils: one for assuring a minimum homogeneous field; and a second coil set working with opposing fields for obtaining a high gradient. Figure 3 shows the details of the magnetic flux density with high saturated areas using Permandur 2V material with the parameters of table 1.

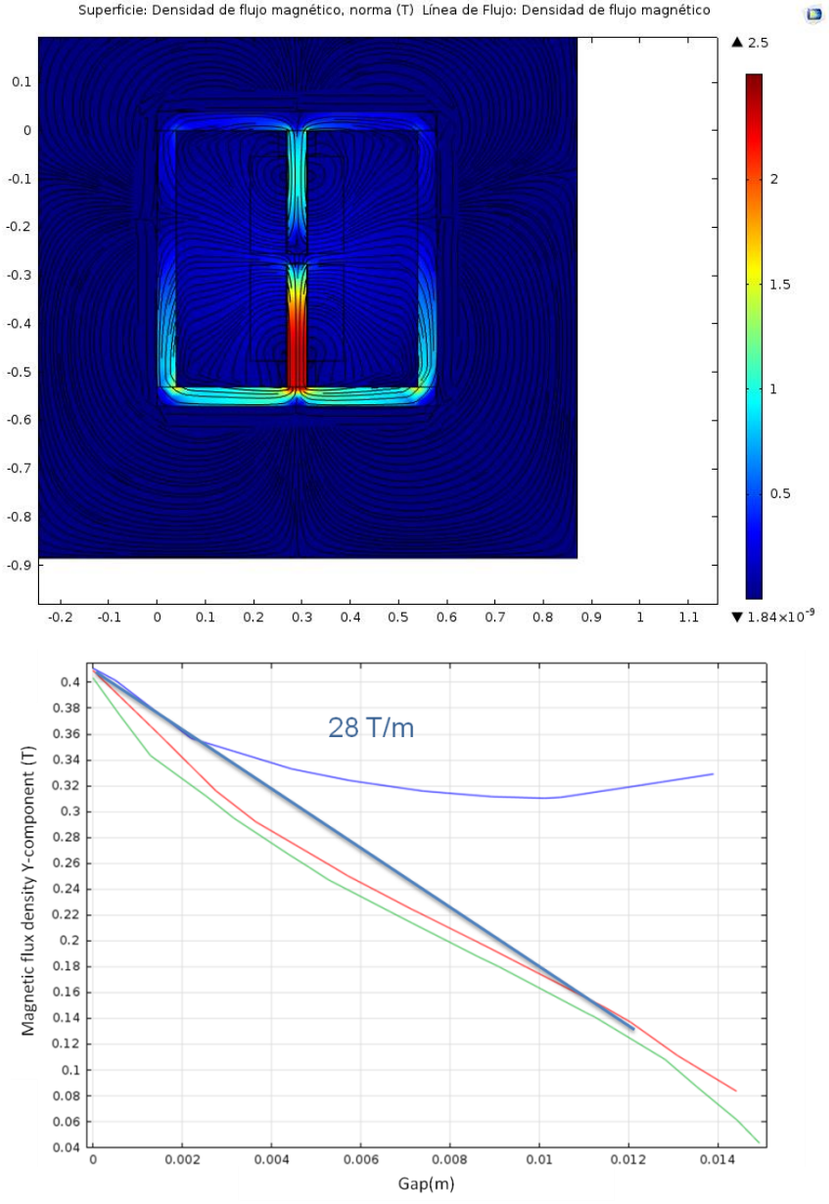

Figure 3. Initial model, which based on reference [18]. In the magnetic flux density diagram, the light blue line shows the evolution of the magnetic flux density along the gap in the middle of the operating area, the green and red lines at both edges of the working area (7.5 mm from the middle line.

Table 1. Summary of the device features.

Geometry	
Operating rage	15x15 mm
Core section	40x40 mm
Electrical parameters	
Number of coils	4
Turns	431 turns/coil (magnetizing coils), 190 turns coil (gradient coil)
Material of the magnetic core	Permandur 2V

Given the high saturation and required power, the design concept changed from using the magnetizing-gradient coils approach to only using the geometry of the poles to obtain the desired flux pattern. In order to separate the heat source from the working area and reducing the power consumption, the second concept in the middle of Figure 2 was evaluated. In that case, it was possible to reach at 30 T/m in certain areas aligning the fields generated at the coils at both side arms. As the gradient is obtained without opposing fields, and it is a result of the design of the magnetic circuit, the required power is also lower. Unfortunately, the obtained pattern was not regular enough, as it can be seen in Figure 4, using the parameters of table 2. The details of the final design are given in the next subsections.

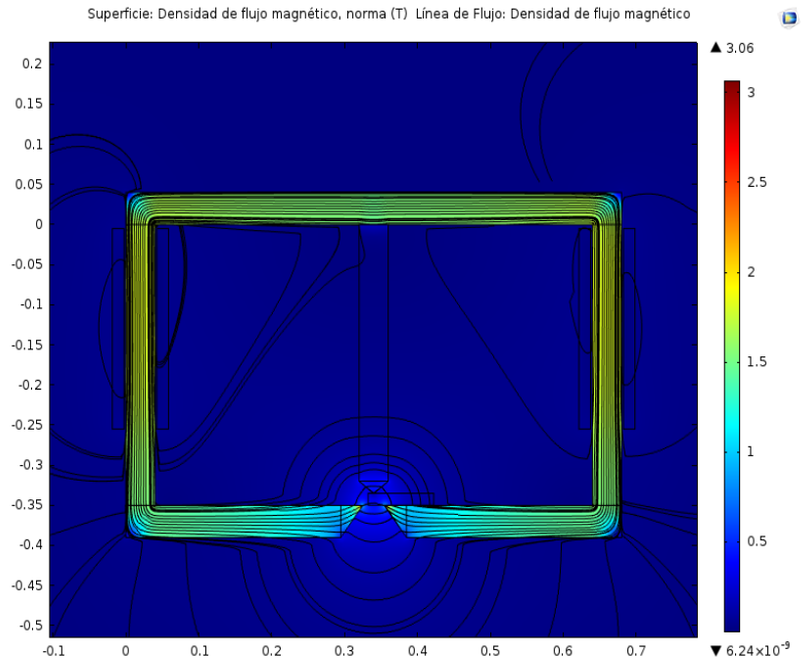

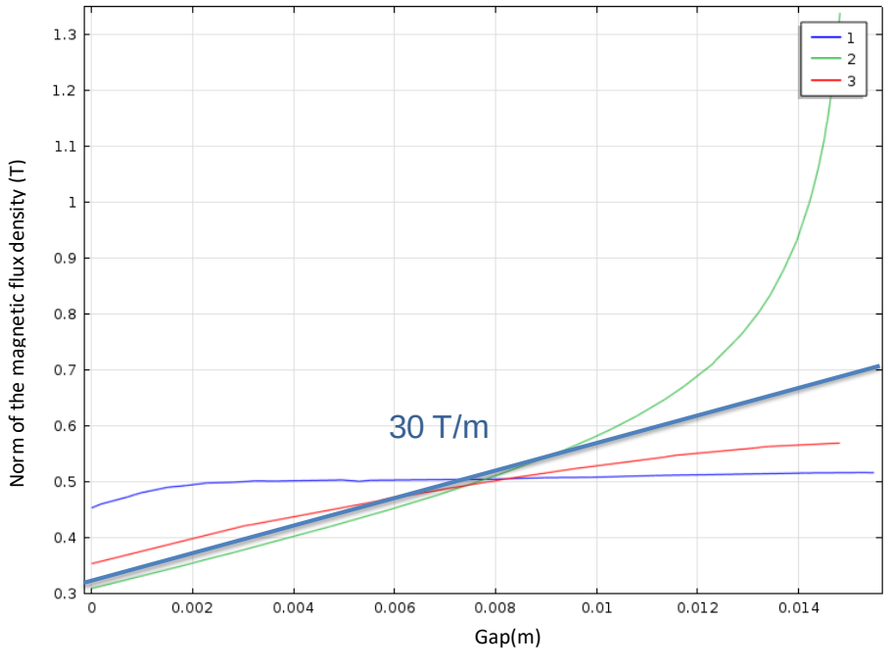

Figure 4. The magnetic flux density diagram of the intermediate design of Figure 2. The blue line (1) shows the evolution of the magnetic flux density along the gap in the middle of the operation area, the green line (2) at +/-7.5 mm while the red line (3) at +/-15mm.

Table 2. Summary of the device features.

Geometry	
Operating rage	15x15 mm
Core section	40x40 mm
Electrical parameters	
Number of coils	2
Turns	380 turns/coil
Material of the magnetic core	M330 - 50 A

An evolution of the geometry of the poles of that intermediate design (adjustment of the distance between the poles to avoid local perturbations) is the last design, on the bottom right-hand side of Figure 2. In that case, it was possible to maintain the separation of the heat sources from the sample. Besides, mirroring the design in a symmetrical structure permitted to magnetize in two different directions and maintain regular field gradients in the working area. This last design is the one which finally selected. The summary of its features is listed in table 3.

Description of the chosen concept

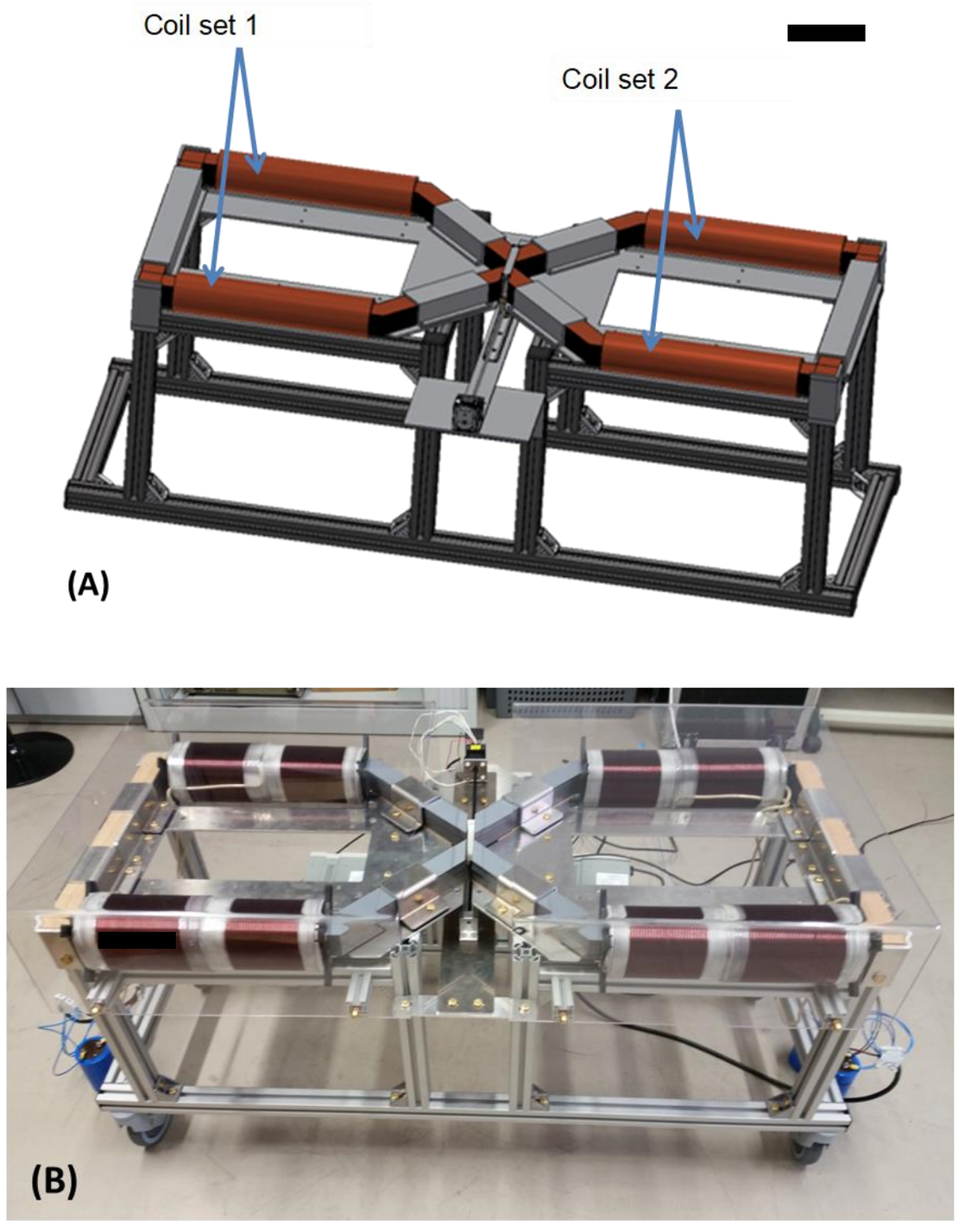

Figure 5. Model (A) and real (B) structure of the device of magnetic field generation. Both scale bars are equivalent to 15 cm.

The designed device (Figure 5) consisted of:

- The magnetic circuit made out of two modules (left and right) which can be sequentially connected in order to generate forces in one direction or another.

- A displacement actuator which locates the sample in the gap between the two modules. The samples are located in a row and the actuator moves them to sequentially place them in the operating area. This way it is possible to change the sample that is affected by the magnetic field. The system may work with up to 3 samples.
- The controller has two separate elements: on the one hand, the movement of the samples; and on the other hand, the generation of an alternating magnetic field. In the first case, a position control is used for commanding a stepper Elmeq motor (MLI1FRL17A4-EQ-LB3M180GT) connected to a mechanical spindle. In the second case, the current command is given by a signal generator GWInstek PSB 2800L, which control two power sources GW-Instek AFG-2225.

Operating principle

The force on a magnetized particle *m* can be described by the equation below:

$$F = m\nabla B$$

where,

m: magnetic moment of the particle ($A{\cdot}m^2$)

B: magnetic flux density (T)

In order to design the system, a model-based approach was followed. A 2D finite element representation was used to design and verify the different designs. The software *Comsol Multiphysics* © was used as simulation environment.

Figure 6 shows the value of B in the magnetic material and in the surrounding space air when the two coils of one side are connected at the same time to obtain a single direction force (results obtained when the upper coils are powered with 30 A).

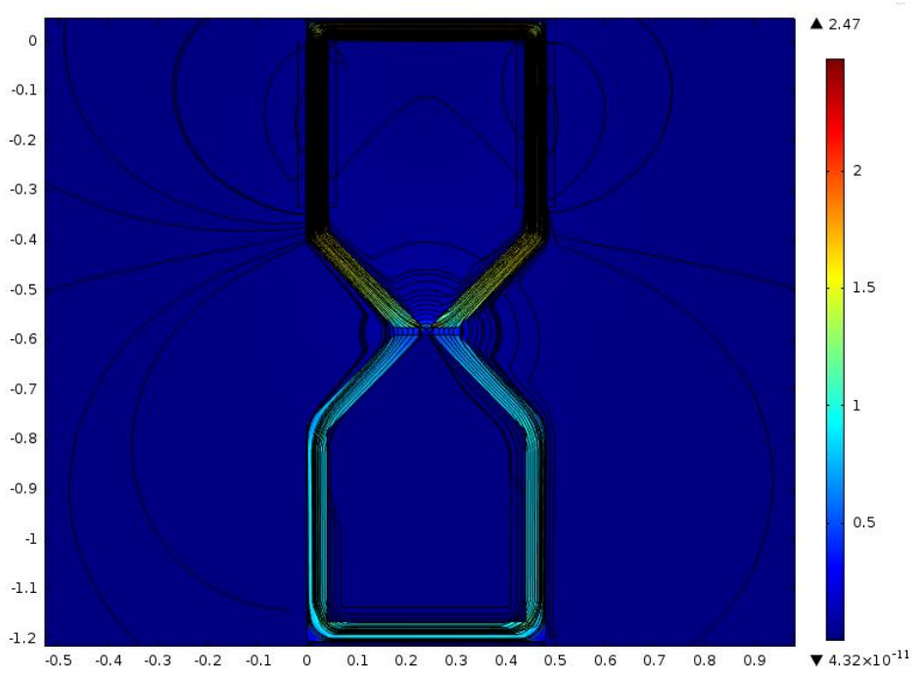

Figure 6. The value of the magnetic flux density (T) in the space when two coils of one side are connected at the same time.

Figure 7 shows the gradient of the magnetic flux. The red line shows the evolution of the magnetic flux density along the gap in the middle of the operation area, the green line at the edge of the working area (7.5 mm from the middle line), and the blue line at 15 mm of the central line, therefore outside the working area. As it can be observed, the distribution in the center of the graph has an almost constant gradient and a similar pattern appears at the edge of the working area. Outside it, the gradient is significantly reduced. In consequence, the irradiated area is confined in the working area.

As previously described, the control system can separately modify the current in both coil sets. In this way, it is possible to change the magnetizing sign, the gradient value and the duration of the magnetic field affecting each tested sample. Magnetic field magnitude in central point of the designed device was measured by a gaussmeter 4048CE (FW Bell, USA).

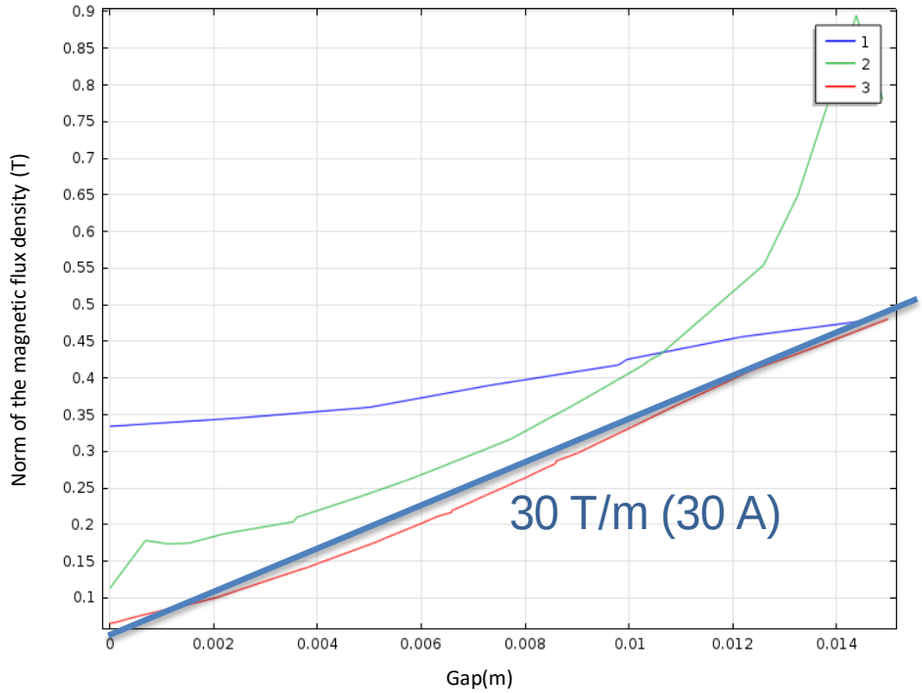

Figure 7. The gradient of the magnetic flux density (B) @30 A in one side (magnetic flux density 1: at 30 mm of the central line; 2: at 15 mm, and 3: at the central line).

The features of the device are summarized in the table 3:

Table 3. Summary of the device features.

Geometry	
Operating rage	15x15 mm
Core section	40x40 mm
Dimension of the complete device (width/length)	480x1180 mm
Electrical parameters	
Number of coils	4
Turns	380 turns/coil
Operating mode	Groups of two alternatively working
Resistance of each coil	0.1 Ω
Inductance of each coil	117 mH
Power consumption with the highest flux gradient	90 W/coi
Material of the magnetic core	M330 - 50 A
Magnetic performance	
Magnetic flux gradient	30 T/m

Central point magnetic flux magnitude	245 mT

Particle synthesis

PLA-ferromagnetic particles were synthesized according to Clara-Trullillo et al. 22 in order to validate the device properties. Briefly, 5 % w/w ferrite nanoparticles (MNPs EMG1300; Ferrotec Ferrofluid, USA) was added to non-aqueous phase composed by 2 % w/v PLA-chloroform solution. The aqueous phase was a solution of 4 % w/v PVA in MilliQ water. Then, 20 mL of PLA/chloroform solution was added using a syringe pump (New Era Pump Systems Inc., USA) to 200 mL aqueous phase in an emulsion-agitator container under 150 rpm agitation (flow rate = 1 mL/min). After 24 h, particles were washed 4 times with deionized water, 50 µm diameter sieved, lyophilized (LyoQuest 85, Telstar, Spain) for 48 h and finally, plasma treated (Plasma Electronic, Germany).

Biological experimentation

Cell culture and microtissue formation

Human dental pulp stem cells (hDPSC) (Lonza, Switzerland) were cultured in proliferation media, containing alpha Minimum Essential Media (αMEM) (Gibco, USA) supplemented with 10 % fetal bovine serum (FBS) (Gibco), 1 % penicillin-streptomycin antibiotic solution (Gibco) and 2 mM L-glutamine (Gibco) [23], and cultured in 75 cm^2 culture flasks in a humidified atmosphere at 37° C, 5 % CO_2 and 95 % air. The passage number of cells used in this study was 3 to 5. Culture media was changed every 2-3 days.

Cultured cells were detached with Trypsin-EDTA solution (Gibco, USA), resuspended in cell culture media and cell density was measured using an EVE Automated Cell Counter (Bio-Rad Laboratories, USA). Cell suspension was centrifuged and $6x10^5$ cells in 300 µL of cell culture media were aliquoted in 0.5 mL microcentrifuge tubes and cultured for 3 days to obtain compact pellets or microtissues.

Irradiation treatment

A magnetic field of 245 T with a pulse direction changing every 3 seconds was applied for 2 cycles of 20 min irradiation/40 min resting time, twice a day, for 3 days. Samples were placed at the centre of the magnetic device during irradiation treatment (A-treated samples). For the whole treatment duration, control non-irradiated samples were either kept outside the cell incubator at 37° C (B-control) or at room temperature (C-control) during the same time of group A-samples treatment, whereas a third control non-irradiated samples were maintained inside the cell

incubator (D-control). During the periods of irradiation treatment, the microcentrifuge tubes of all groups were kept closed, whereas when daily treatment finished, the tubes were opened inside the incubator so that CO_2 and O_2 gases are equilibrated until the next irradiation period.

Cell viability

After 3 days of electromagnetic stimulation treatment, cellular viability was assessed. Cytotoxicity assay (MTS) (Promega, Spain) was carried out on A-treated samples and B-, C- and D-controls following manufacturer's instructions. Cellular microtissues were centrifuged and resuspended in 100 µL media without phenol red, transferred to 96-well culture plate and incubated with 20 µL of MTS assay reagent for 2 h at 37° C. The quantity of formazan product originated by mitochondrial metabolism of cultured cells was measured by absorbance at 490 nm using a Victor X3 2030 Multilabel Reader (PerkinElmer, USA). The absorbance values obtained after blank subtraction are directly proportional to the number of viable cells.

Morphological study

To study cell morphology, one microtissue for each sample and control condition was washed with 300 µL of ice-cold phosphate buffered saline (PBS) (Euroclone, Italy) twice for 5 min, fixed with 4 % formaldehyde (VWR Chemicals, Prolabo, Germany) for 20 min, resuspended in 100 µL of PBS and layered on a glass slide using a Cytospin 3 (Thermo Shandon, USA). Samples were dried at room temperature and sequentially stained with Papanicolaou's hematoxylin solution (Merck, Germany) and 1 % eosin (Merck) for 2 and 1 min, respectively. Finally, samples were observed in a bright-field microscope (Leica DMLB).

RESULTS

Validation of the magnetic device

The validation was done by using synthesized PLA-ferromagnetic particles between 30 and 50 µm of diameter.

These particles were dispersed in a solution of 1 % ethylene glycol in water, transferred to a microcentrifuge tube, and then located in the working area of the magnetic device. In these conditions and considering a mean particle size of 40 µm, their properties were:

- the viscosity of the fluid is approximated by 0.002141 Pa.s using the volume percentage among ethylene glycol and water,
- the new particles have a magnetic moment of 4.67×10^{-10} Am^2,

- the expected viscous coefficient for the particle in such fluid, according to the Stokes law, is 1.61×10^{-6} Ns/m,
- mass of 5.11×10^{-11} kg,
- the expected force level with a gradient of the magnetic flux of 30 T/m is 14 nN.

Figure 8 shows the expected evolution for a particle of 40 µm of the position with time calculated using Newton Law:

$$F = m_p \frac{d^2}{dt^2} x + c \frac{d}{dt} x$$

With *F,* the magnetic force, m_p the mass of the particle and *c* the viscosity of the fluid. The displacement is:

$$x = \frac{F}{c} t + \frac{m_p}{c^2} F\left(1 - e^{(-c/m_p * t)}\right)$$

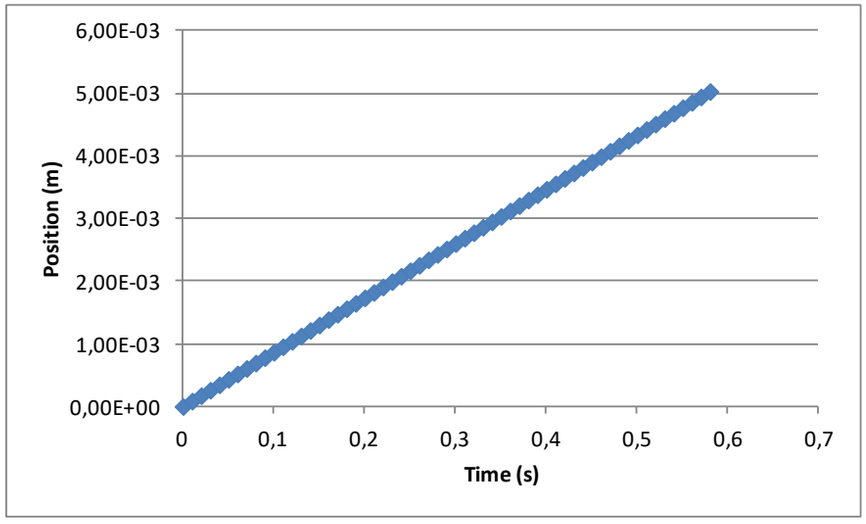

Figure 8. Typical position evolution for a 40 µm particle.

As observed in Figure 8, a terminal speed of 8.7 mm/s was obtained for a reference 40 µm particle.

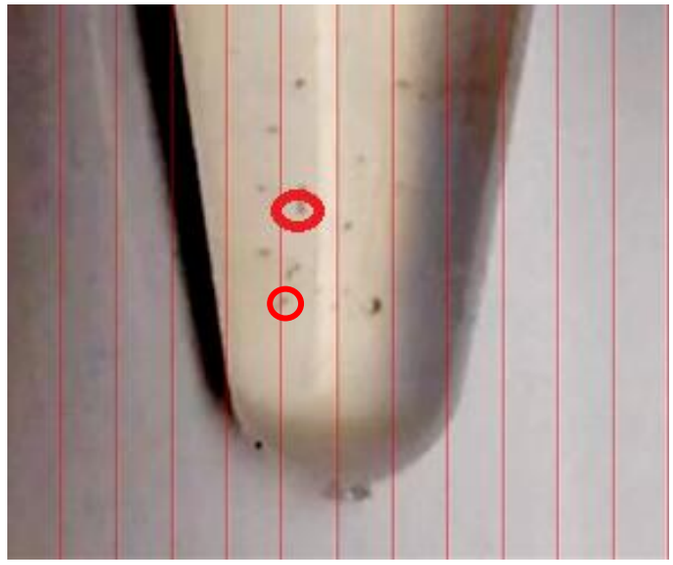

Figure 9. The image shows the bottom of a microfuge tube containing PLA-ferrite microparticles. Highlighted reference particles 1 -down- and 2 -up- are selected for the displacement measurement. The vertical lines represent 1 mm partition. The image is taken from one of the recorded videos.

In order to validate the operation of the device, the movement of the framed particles in the Figure 9 was repeatedly measured in a range of 3 mm resulting in the values displayed in Figure 10. As it can be seen, the measured values match the expected result for particles between 30 and 50 µm diameter.

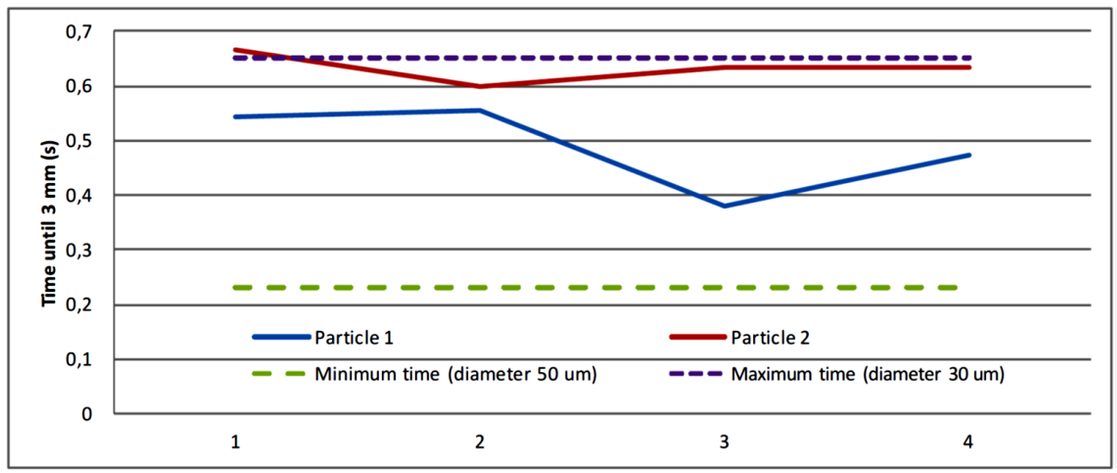

Figure 10. Measured times for particles 1 and 2 at several tests. (accuracy of the time measurement +/- 0.1 s)

Biological results

Cell viability

After 3 days of irradiation treatment period, irradiated cells (A-samples) showed a 59 % increase on relative absorbance when compared to non-irradiated B- to D-control groups (Figure 11), whereas no differences were found between all control groups. Since the initial number of seeded cells was the same ($6x10^5$ cells) for all the groups, the increase in absorbance observed in the irradiated samples means an increase in the number of viable cells after 3 days of treatment.

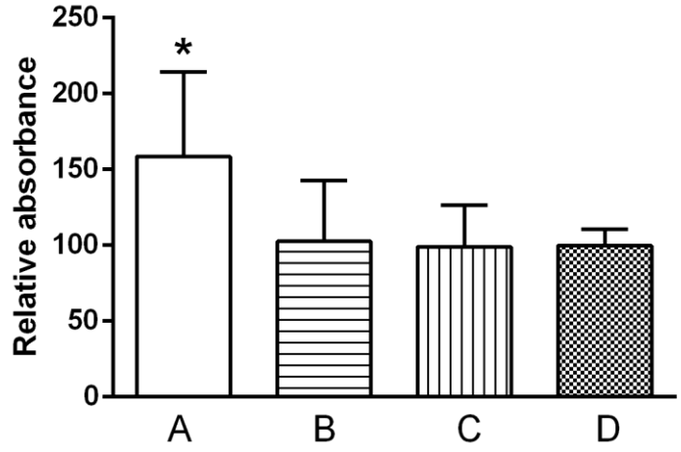

*Figure 11. Viability study of A-treated and B-, C- and D-control samples after 3 days of treatment. Values represent the percentage of absorbance with respect to D-control group. Mean ± SD; *p ≤ 0.05 with respect to D-control group.*

Morphological study

After hematoxylin and eosin staining (Figure 12), cells from all groups were observed isolated or in small groups, and presented a polygonal shape with scarce, short processes with a round centric or eccentric basophil nucleus with dense chromatin, and homogeneously stained eosinophil cytoplasm. These morphological characteristics were similar to those reported for mesenchymal dental pulp stem cells in culture [19,23]. No morphological differences were found between irradiated cells (A-samples) and control groups. Therefore, no significant morphological differences were found in the different groups, but a higher cell density was observed in A-samples, which agrees with the viability assay results exposed above.

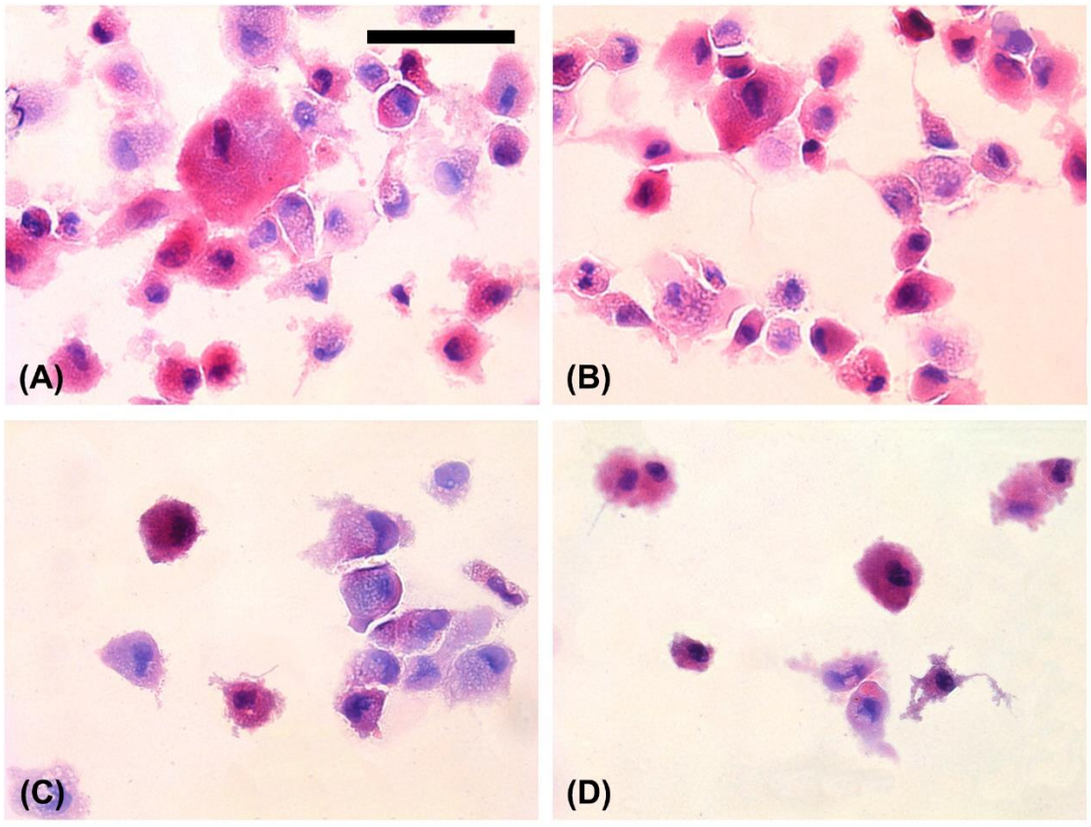

Figure 12. Hematoxylin-eosin staining of A-treated samples after 3 days of irradiation, and B-C- and D-control samples. Bright-field microscopy images. Scale bar = 50 µm.

DISCUSSION

Recent studies are focused on the use of electromagnetic fields to induce cell proliferation and differentiation, that would finally improve the repair of tissue defects caused by diseases such as osteoarthritis [20,24,25]. A wide range of electromagnetic field and exposure time values has been used, but many studies apply an exposure in the range of mT and below, and an exposure time of 1 h. In this work, the magnetic field used was 245 mT, close to the 600 mT used by Suryani *et al*. [20] or by Negi *et al*. [24], while 4 daily irradiations of 20 min each for 3 days were established to study stimulation effect on cells. Suryani *et al*. [20] studied the effect of different exposure times per day and showed that 15 min of exposure originated an increase in the content of DNA and RNA in the irradiated samples, that means an induction in cell proliferation *in vitro*. However, Negi *et al*. reduced the exposure time to 10 min daily and found no differences between irradiated and control samples [24]. Moreover, Ribeiro *et al*. [25] showed a 25 % increase in cell proliferation in electromagnetically- and mechanically-stimulated samples with respect to non-mechanically stimulated cells. Therefore, the irradiation treatment designed in this study was 4 x 20 min daily for 3 days, which showed an increase of more than 50 % in cell content in

electromagnetically-irradiated samples compared to non-irradiated control samples. In this case, the magnitude of the electromagnetic field did not affect cell content, but the exposure time was responsible for that change.

Respect to cell morphology, Negi's exposure treatment showed that mesenchymal stem cells did not undergo malignant transformation or formation of colonies when cells were cultured in soft agar [24], whereas the irradiation parameters applied by Ribeiro *et al.* showed no significant differences in cell morphology between stimulated and control samples [25], and similarly the irradiation treatment of this study showed similar morphology in all groups of samples (irradiated and controls), with polygonal cells with scarce and short processes, with rounded nuclei of dense chromatin and homogeneously stained eosinophil cytoplasm. These cell morphological characteristics were similar to that of hDPSC cultured in 3D scaffolds as alginate beads, as previously described by our group [19].

Exposure to the electromagnetic field did not alter the morphology of mesenchymal stem cells but increased cell number, probably inducing cell proliferation, which is a goal of different trauma treatments [26] where cells are implanted in chondral lesions [27,28] and thus a high content of cells is required.

The obtained results with the designed device confirm those presented in the literature regarding the positive effect of the irradiation in the cell proliferation with tests showing an increased number of cells without morphological differences compared to non-irradiated samples. Apart from asserting previous results, there is a remarkable difference between the tests described in the literature, which are focused on constant fields, and the test performed with the designed device, which applies a strong and changing field gradient. It has been very interesting to observe that even a dynamically changing configuration does not cause observable asymmetries in cell growth. Although previous tests seemed to show the independence of the cell growth with the field magnitude, the results obtained in the present work also shows no effect derived from dynamic field gradients. This fact opens up the possibility of combining the effects of mechanical excitation by adding magnetic beads and irradiation.

CONCLUSIONS

We have described, developed and fabricated an electromagnetic device for irradiating biological samples and for generating forces without contact in magnetic particles. The designed system can produce a regular magnetic gradient of about 30 T/m in a working area of 15x15 mm. These values are well above the normal operating range of other magnetic tweezers of similar electric power, which are normally focused on smaller irradiation areas. This device has

been experimentally evaluated in two different conditions: irradiating biological samples from human dental pulp stem cells and mechanically moving magnetic nanoparticles. The second test was used for validating the theoretical values of the generated magnetic field.

The irradiated biological samples showed higher cellular content than control groups (kept into cell incubator or outside cell incubator at 37° C or at room temperature during irradiation treatment), whose viability was similar. As expected, the cells showed morphological characteristics of dental pulp stem cells, but no differences were found between irradiated cells and control group. As a summary, the exposure to the electromagnetic field did not alter the morphology of mesenchymal stem cells but increased its number.

In conclusion, the device described in the present paper has proven its functionally for magnetic irradiation of samples and for the generation of mechanical stimuli through magnetic forces on ferric particles.

Acknowledgements

The authors gratefully acknowledge the financial support from the Spanish Ministry of Science and Innovation (PID2019-106099RB-C44 and PID2019-106099RB-C42 / AEI / 10.13039/501100011033), the Government of Aragon (DGA-T24_20R) and the Biomedical Research Networking Center in Bioengineering, Biomaterials and Nanomedicine (CIBER-BBN). CIBER-BBN is financed by the Instituto de Salud Carlos III with assistance from the European Regional Development Fund.

Data Availability

The data that supports the findings of this study are available within the article.

BIBLIOGRAPHY

[1] D. Desmaële, M. Boukallel, and S. Régnier, J. Biomech. **44**, 1433 (2011).

[2] T.U. Eindhoven, *Magnetic Particle Actuation for Functional Biosensors Door* (2009).

[3] S.J. Mousavi and M.H. Doweidar, Comput. Mech. **63**, 471 (2019).

[4] R.H.W. Funk, T. Monsees, and N. Özkucur, Prog. Histochem. Cytochem. **43**, 177 (2009).

[5] M.S. Markov, Electromagn. Biol. Med. (2007).

[6] K. Lim, J. Hexiu, J. Kim, H. Seonwoo, W.J. Cho, P.H. Choung, and J.H. Chung, Biomed Res. Int. (2013).

[7] C. Cunha, S. Panseri, M. Marcacci, and A. Tampieri, Am. J. Biomed. Eng. **2**, 263 (2013).

[8] S.J. Mousavi and M.H. Doweidar, Comput. Methods Programs Biomed. **130**, 106 (2016).

[9] J. Huegel, D.S. Choi, C.A. Nuss, M.C.C. Minnig, J.J. Tucker, A.F. Kuntz, E.I. Waldorff, N. Zhang, J.T. Ryaby, and L.J. Soslowsky, J. Shoulder Elb. Surg. **27**, 553 (2018).

[10] N. Bloise, L. Petecchia, G. Ceccarelli, L. Fassina, C. Usai, F. Bertoglio, M. Balli, M. Vassalli, M.G. Cusella De Angelis, P. Gavazzo, M. Imbriani, and L. Visai, PLoS One **13**, e0199046 (2018).

[11] R. El-Ayoubi, C. DeGrandpré, R. DiRaddo, A.-M. Yousefi, and P. Lavigne, J. Biomater. Appl. **25**, 429 (2011).

[12] M. Keller, J. Schilling, and E. Sackmann, Rev. Sci. Instrum. **72**, 3626 (2001).

[13] A.H.B. de Vries, B.E. Krenn, R. van Driel, and J.S. Kanger, Biophys. J. **88**, 2137 (2005).

[14] X. Wang, C. Ho, Y. Tsatskis, J. Law, Z. Zhang, M. Zhu, C. Dai, F. Wang, M. Tan, S. Hopyan, H. McNeill, and Y. Sun, Sci. Robot. (2019).

[15] Zhipeng Zhang, Kui Huang, and Chia-Hsiang Menq, IEEE/ASME Trans. Mechatronics **15**, 704 (2010).

[16] H. Huang, C.Y. Dong, H.-S. Kwon, J.D. Sutin, R.D. Kamm, and P.T.C. So, Biophys. J. **82**, 2211 (2002).

[17] F. Amblard, B. Yurke, A. Pargellis, and S. Leibler, Rev. Sci. Instrum. (1996).

[18] C. Haber and D. Wirtz, Rev. Sci. Instrum. **71**, 4561 (2000).

[19] M. Mata, L. Milian, M. Oliver, J. Zurriaga, M. Sancho-Tello, J.J.M. de Llano, and C. Carda, Stem

Cells Int. **2017**, 1 (2017).

[20] L. Suryani, J.H. Too, A.M. Hassanbhai, F. Wen, D.J. Lin, N. Yu, and S.H. Teoh, Tissue Eng. - Part C Methods **25**, 114 (2019).

[21] INCOSE, *Systems Engineering Handbook: A Guide for System Life Cycle Processes and Activities* (2007).

[22] S. Clara-Trujillo, J.C. Marín-Payá, L. Cordón, A. Sempere, G. Gallego Ferrer, and J.L. Gómez Ribelles, Colloids Surfaces B Biointerfaces **177**, 68 (2019).

[23] R.S. Clavell, J.J.M. de Llano, C. Carda, J.L.G. Ribelles, and A. Vallés-Lluch, J. Biomed. Mater. Res. - Part A **104**, 2723 (2016).

[24] H. Negi, S. Takeuchi, N. Kamei, S. Yanada, N. Adachi, and M. Ochi, Tissue Eng. - Part C Methods **25**, 324 (2019).

[25] C. Ribeiro, V. Correia, P. Martins, F.M. Gama, and S. Lanceros-Mendez, Colloids Surfaces B Biointerfaces (2016).

[26] L. Martinez-Riaza, H. Herrero-Gonzalez, J.M. Lopez-Alcorocho, P. Guillen-Garcia, and T.F. Fernandez-Jaen, BMJ Open Sport Exerc. Med. **2**, 4 (2017).

[27] P. Guillén-García, E. Rodríguez-Iñigo, I. Guillén-Vicente, R. Caballero-Santos, M. Guillén-Vicente, S. Abelow, G. Giménez-Gallego, and J.M. López-Alcorocho, Cartilage **5**, 114 (2014).

[28] J.M. Lopez-Alcorocho, L. Aboli, I. Guillen-Vicente, E. Rodriguez-Iñigo, M. Guillen-Vicente, T.F. Fernández-Jaén, S. Arauz, S. Abelow, and P. Guillen-García, Cartilage **9**, 363 (2018).